Cisplatin−DNA Cross-Link Retro Models with a Chirality-Neutral Carrier Ligand: Evidence for the Importance of "Second-Sphere Communication"

Sharon T. Sullivan,[‡] Antonella Ciccarese,[†] Francesco P. Fanizzi,[†,§] and Luigi G. Marzilli*[,‡]

Dipartimento di Biologia, Università di Lecce, Via Monteroni, I-73100 Lecce, Italy, Cancer Research Center, Consortium C.A.R.S.O., I-70010 Valenzano-Bari, Italy, and Department of Chemistry, Emory University, Atlanta, Georgia 30322

Received July 3, 2000

We employ retro models, *cis*-PtA_2**G**$_2$ (A_2 = a diamine, **G** = guanine derivative), to assess the cross-linked head-to-head (HH) form of the cisplatin−DNA d(GpG) adduct widely postulated to be responsible for the anticancer activity. Retro models are designed to have minimal dynamic motion to overcome problems recognized in models derived from cisplatin [A_2 = $(NH_3)_2$]; the latter models are difficult to understand due to rapid rotation of **G** bases about the Pt−N7 bond in solution and the dominance of the head-to-tail (HT) form in the solid. Observation of an HH form is unusual for *cis*-PtA_2**G**$_2$ models. Recently, we found the first HH forms for a *cis*-PtA_2**G**$_2$ model with A_2 lacking NH groups in a study of new **Me$_2$ppz**Pt**G**$_2$ models. (**Me$_2$ppz**, *N*,*N*′-dimethylpiperazine, has in-plane bulk which reduces dynamic motion by clashing with the **G** O6 as the base rotates into the coordination plane from the ground state position approximately perpendicular to this plane. **G** = 5′-GMP and 3′-GMP.) The finding of an HH form (albeit in a mixture with HT forms) with both **G** H8 signals unusually downfield encouraged us to study additional **Me$_2$ppz**Pt**G**$_2$ analogues in order to explain the unusual spectral features and to identify factors that influence the relative stability of HT and HH forms. Molecular modeling techniques suggest HH structures with the H8's close to the deshielding region of the *z* axis of the magnetically anisotropic Pt atom, explaining the atypical shift pattern. When **G** = 1-Me-5′-GMP, we obtained NMR evidence that the HH rotamer has a high abundance (34%) and that the three rotamers have nearly equal abundance. These findings and the observation that the relative HT distributions varied little or not at all as a function of pH when **G** = Guo, 1-MeGuo, or 1-Me-5′-GMP are consistent with two of our earlier proposals concerning phosphate groups in HT forms of *cis*-PtA_2(GMP)$_2$ complexes. We proposed that a **G** phosphate group can form hydrogen bonds with the cis **G** N1H ("second-sphere" communication) and (for 5′-phosphate) A_2 NH groups. The new results with 1-Me-5′-GMP led us to propose a new role for a 5′-phosphate group; it can also favor the HH form by counteracting the natural preference for the **G** bases to adopt an HT orientation. Finally, the HH form was also sufficiently abundant to allow observation of a distinct ^{195}Pt NMR signal (downfield of the resonance observed for the HT forms) for several complexes. This is the first report of an HH ^{195}Pt NMR signal for *cis*-PtA_2**G**$_2$ complexes.

Introduction

Cisplatin (*cis*-Pt$Cl_2(NH_3)_2$) is a drug that is successful in the treatment of a number of cancers.[1,2] Cisplatin targets DNA, most frequently binding at the N7 atoms of adjacent guanines (G's).[1−6] This intrastrand adduct is thought to be the lesion responsible for cell death, although the mechanism of action is not entirely understood. The search for a more active drug has prompted strong interest in the development and screening of a large number of cisplatin analogues (*cis*-PtX_2A_2, A_2 = two unidentate or one bidentate amine ligand). Although no analogues with other carrier ligands have gained wide clinical use, good activity was exhibited by derivatives with A_2 = primary or secondary amines. This observation led to speculation concerning the importance of the hydrogen-bonding capability of the amine NH's of the carrier ligand.[2,7,8] Such hydrogen bonding may be important for the stabilization of DNA distortions caused by formation of the intrastrand cross link.[8] On the other hand, amines lacking NH groups have bulk projecting out of the coordination plane,[9−12] possibly clashing with the G O6 atom. Such clashes could lead to distortions in DNA different from those caused by Pt compounds with less bulky NH-bearing carrier ligands.

* To whom correspondence should be addressed. E-mail: lmarzil@emory.edu.
† Università di Lecce.
§ Consortium C.A.R.S.O.
‡ Emory University.

(1) Reedijk, J. *Chem. Commun.* **1996**, 801−806.
(2) Bloemink, M. J.; Reedijk, J. In *Metal Ions in Biological Systems*; Sigel, A., Sigel, H., Eds.; Marcel Dekker: New York, 1996; Vol. 32, pp 641−685.
(3) Sherman, S. E.; Lippard, S. J. *Chem. Rev.* **1987**, *87*, 1153−1181.
(4) Kline, T. P.; Marzilli, L. G.; Live, D.; Zon, G. *J. Am. Chem. Soc.* **1989**, *111*, 7057−7068.
(5) Fouts, C.; Marzilli, L. G.; Byrd, R.; Summers, M. F.; Zon, G.; Shinozuka, K. *Inorg. Chem.* **1988**, *27*, 366−376.
(6) Iwamoto, M.; Mukundan, S., Jr.; Marzilli, L. G. *J. Am. Chem. Soc.* **1994**, *116*, 6238−6244.
(7) Cleare, M. J.; Hydes, P. C. In *Metal Ions in Biological Systems*; Sigel, H., Ed.; Marcel Dekker: New York, 1980; Vol. 11, pp 2−62.
(8) Natile, G. *Metal-Based Drugs* **1994**, *1*, 311−319.
(9) Cramer, R. E.; Dahlstrom, P. L. *J. Am. Chem. Soc.* **1979**, *101*, 3679−3681.
(10) Marcelis, A. T. M.; Van der Veer, J. L.; Zwetsloot, J. C. M.; Reedijk, J. *Inorg. Chim. Acta* **1983**, *78*, 195−203.
(11) Carlone, M.; Fanizzi, F. P.; Intini, F. P.; Margiotta, N.; Marzilli, L. G.; Natile, G. *Inorg. Chem.* **2000**, *39*, 634−641.
(12) Elizondo-Riojas, M.-A.; Kozelka, J. *Inorg. Chim. Acta* **2000**, *297*, 417−420.

10.1021/ic000736x CCC: $20.00
Published on Web 12/21/2000

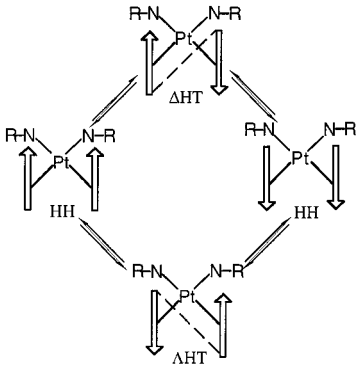

Figure 1. Schematic representation of the interconversion between HT and HH atropisomers of *cis*-PtA_2**G**$_2$ (A_2 = **Me$_2$ppz**) complexes viewed with the **G** coordination sites forward and piperazine ligands to the rear (mostly omitted for clarity). Arrows represent the **G** bases with H8 at the head. The two possible HT rotamers are differentiated by an imaginary line (dotted line in this figure) drawn between the O6 atoms of each of the **G** ligands. The resulting line (viewed from the **G** side of the coordination plane) has either a positive slope (ΔHT) or a negative slope (ΛHT). R = CH_3 when A_2 = **Me$_2$ppz**.

Differences between carrier ligands may lead to populations of conformers other than the head-to-head (HH) conformer (Figure 1) favored by the cisplatin−DNA intrastrand cross-linked adduct.[4,5,13,14] In contrast to the DNA adducts, a head-to-tail (HT) form (Figure 1) is often observed to dominate in *cis*-PtA_2**G**$_2$ (boldface **G** = unlinked guanine derivative) cross-link models, while the HH form is less favored and less frequently observed.[9,15−19] Interconversion between the HH and HT conformations is possible via rotation of the Pt−**G** N7 bond in *cis*-PtA_2**G**$_2$ complexes. For adducts derived from cisplatin itself, these processes are rapid on the NMR time scale, and the simplicity of the *cis*-Pt$(NH_3)_2$ drug moiety makes it difficult to elucidate the chemistry. Therefore, we use retro models, adducts in which the carrier ligand (A_2) is more complicated than the *cis*-$(NH_3)_2$ ligands.[14,15,17,18] The A_2 groups in retro models are usually bulky; the use of bulky A_2 groups slows rotation about the Pt−**G** N7 bond and allows observation of the different HT and HH atropisomers by NMR spectroscopy.[15,17,20,21] The number of observable NMR signals for *cis*-PtA_2**G**$_2$ complexes is determined by the local symmetry of the *cis*-PtA_2 moiety and the asymmetry of the **G** ribose residue. For a *cis*-PtA_2**G**$_2$ complex with a C_2-symmetrical *cis*-PtA_2 moiety and a **G** containing a sugar residue, observation of up to four ^{1}H NMR signals for each proton type is possible [one for each HT form (Δ and Λ) and two signals of equal intensity for the HH form]. Generally, the **G** H8 NMR signal alone can be used to identify conformers since it is in an isolated region and exhibits the greatest dependence on conformation.

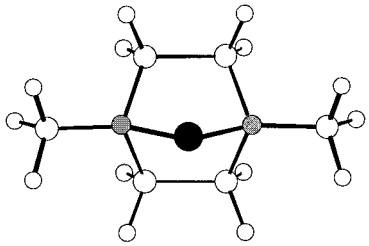

Figure 2. Ball-and-stick model of the cisplatin analogue, [dichloro(*N*,*N*′-dimethylpiperazine)platinum(II)], showing the Pt(**Me$_2$ppz**) moiety (Pt atom is black, and N atoms are shaded).

The platinum carrier ligand, *N*,*N*′-dimethylpiperazine (**Me$_2$ppz**, Figure 2)[22] studied here is unique since it lacks chirality and any axial or equatorial NH or alkyl groups.[15,17] We refer to **Me$_2$ppz** as a chirality-neutral chelate (**CNC**) ligand on the basis of these characteristics.[22] Furthermore, positioning of the methyl groups in the coordination plane, a special feature designed into this ligand, renders **Me$_2$ppz**Pt**G**$_2$ models less dynamic than typical models, including those derived from cisplatin. The reduced dynamic nature of **Me$_2$ppz**Pt**G**$_2$ complexes allows assessment and potential identification of factors relevant to the relative stabilities of different atropisomers. Carrier ligands lacking NH groups typically have bulk projecting out of the coordination plane.[9−12] Consequently, clashes between such carrier ligands and the **G** O6 atom(s) are possible, even when the **G**'s are in the position adopted at equilibrium. The absence of NH groups in the **Me$_2$ppz** ligand eliminates the possibility of hydrogen-bonding interactions with the **G** O6 atom/phosphate group; these have been proposed to be important in the stabilization of different atropisomers observed for other *cis*-PtA_2**G**$_2$ model complexes.[15,17,20,21] Therefore, in the absence of carrier ligand NH−**G** hydrogen bonding, the relative atropisomer stabilities for **Me$_2$ppz**Pt**G**$_2$ complexes are dictated by other interligand interactions. For example, **G** phosphate group−cis **G** N1H hydrogen bonding appeared to stabilize the dominant ΛHT conformer for **Me$_2$ppz**Pt(5′-GMP)$_2$ (5′-GMP = guanosine 5′-monophosphate).[22] Such "second-sphere" interactions have been identified as important factors stabilizing the Λ and Δ HT rotamers in 5′-GMP and 3′-GMP (guanosine 3′-monophosphate) complexes, respectively, of other *cis*-PtA_2**G**$_2$ models.[17,20,23] When the carrier ligand has NH groups, the 5′-phosphate group in 5′-GMP adducts helps to stabilize HT conformers that allow 5′-phosphate group−carrier ligand NH hydrogen bonds to form.[15,17]

The HH conformer was also observed for these **Me$_2$ppz**Pt-(GMP)$_2$ complexes,[22] marking the first report of an HH form for a *cis*-PtA_2**G**$_2$ model in which the A_2 ligand lacks an NH group. As found for other *cis*-PtA_2**G**$_2$ complexes, the HH form is a minor form compared to the HT conformers and is favored more in the 5′-GMP complex than in the 3′-GMP complex.[15−17] The H8 NMR signals of the HH form in other *cis*-PtA_2**G**$_2$ complexes, generally well separated by ∼1 ppm, are positioned on either side of the two HT H8 NMR signals.[15−17] In comparison, the two H8 NMR signals of the HH rotamer for the **Me$_2$ppz**Pt(5′-GMP)$_2$ and **Me$_2$ppz**Pt(3′-GMP)$_2$ complexes are quite unusual. Both are downfield from the HT H8 signals and exhibit a much smaller separation (∼0.05−0.13 ppm).

The unusual spectral features, but near normal atropisomer distribution, for the **Me$_2$ppz**Pt(GMP)$_2$ complexes encouraged

(13) Ano, S. O.; Intini, F. P.; Natile, G.; Marzilli, L. G. *J. Am. Chem. Soc.* **1998**, *120*, 12017−12022.
(14) Ano, S. O.; Kuklenyik, Z.; Marzilli, L. G. In *Cisplatin. Chemistry and Biochemistry of a Leading Anticancer Drug*; Lippert, B., Ed.; Wiley-VCH: Weinheim, 1999; pp 247−291.
(15) Marzilli, L. G.; Intini, F. P.; Kiser, D.; Wong, H. C.; Ano, S. O.; Marzilli, P. A.; Natile, G. *Inorg. Chem.* **1998**, *37*, 6898−6905.
(16) Xu, Y.; Natile, G.; Intini, F. P.; Marzilli, L. G. *J. Am. Chem. Soc.* **1990**, *112*, 8177−8179.
(17) Ano, S. O.; Intini, F. P.; Natile, G.; Marzilli, L. G. *Inorg. Chem.* **1999**, *38*, 2989−2999.
(18) Ano, S. O.; Intini, F. P.; Natile, G.; Marzilli, L. G. *J. Am. Chem. Soc.* **1997**, *119*, 8570−8571.
(19) Kiser, D.; Intini, F. P.; Xu, Y.; Natile, G.; Marzilli, L. G. *Inorg. Chem.* **1994**, *33*, 4149−4158.
(20) Wong, H. C.; Intini, F. P.; Natile, G.; Marzilli, L. G. *Inorg. Chem.* **1999**, *38*, 1006−1014.
(21) Wong, H. C.; Coogan, R.; Intini, F. P.; Natile, G.; Marzilli, L. G. *Inorg. Chem.* **1999**, *38*, 777−787.
(22) Sullivan, S. T.; Ciccarese, A.; Fanizzi, F. P.; Marzilli, L. G. *Inorg. Chem.* **2000**, *39*, 836−842.
(23) Williams, K. M.; Cerasino, L.; Intini, F. P.; Natile, G.; Marzilli, L. G. *Inorg. Chem.* **1998**, *37*, 5260−5268.

this study with modeling techniques along with NMR and CD spectroscopy for other **Me$_2$ppz**Pt**G**$_2$ complexes [**G** = 9-ethylguanine (9-EtG), guanosine (Guo), 1-methylguanosine (1-MeGuo), 1-methylguanosine 5′-monophosphate (1-Me-5′-GMP), 2′-deoxyguanosine 5′-monophosphate (5′-dGMP)] and, for comparison, **Me$_2$ppz**Pt(IMP)$_2$ models (IMP = inosine monophosphate).

Experimental Section

Materials. 1-Me-5′-GMP was prepared as previously described.[24] All other guanine derivatives (**G**), 3′-IMP, and 5′-IMP were obtained from Sigma. The PtCl$_2$(**Me$_2$ppz**) complex (Figure 2) was prepared by a modification[25] of the original method.[26]

^{1}H NMR Spectroscopy. All NMR samples (∼2.5−5 mM in Pt) were prepared in D_2O by treating the chloro complex with 1.7 equiv of $AgNO_3$ in the dark for 8−12 h. After AgCl was removed by filtration, the guanine (or inosine) derivative (∼2 equiv) was added. (Often the **G** or IMP:Pt ratios were slightly higher than 2:1 to ensure complete reaction of Pt.) All ^{1}H NMR studies were performed on a GE Omega 600 MHz instrument. A presaturation pulse was employed to suppress the HOD peak, and the residual HOD peak was used as reference. At least 128 scans were collected in each experiment. Saturation transfer experiments were conducted using a presaturation pulse of 3 s and a pulse delay of 1 s. The appropriate symmetrical positions, as well as the peaks of interest, were irradiated in order to eliminate the possibility of any power spillage effects. Ninety-six scans per block (512 blocks) were collected in a 2D nuclear Overhauser enhancement spectroscopy (NOESY) experiment conducted at 5 °C using a spectral width of 6250 Hz and a 500 ms mixing time. Deuterated nitric acid and sodium hydroxide solutions were used in pH studies.

^{195}Pt NMR Spectroscopy. All samples were prepared as described above but at ∼30−40 mM Pt. Spectra were collected on a GE QE 300 MHz instrument operating at 64.5 MHz (Na_2PtCl_6 external reference; ∼64−80 K scans; pulse width = 8 μs; predelay = 0.1 s).

Circular Dichroism (CD) Spectroscopy. CD samples were prepared from the respective NMR samples and diluted to ∼0.07 mM **G** or IMP with deionized water. Ten acquisitions, collected from 400 to 200 nm on a JASCO J-600 CD spectropolarimeter at a scan speed of 50 nm/min, were averaged to improve signal-to-noise ratios.

Molecular Modeling. Molecular mechanics/dynamics (MMD) calculations were carried out on a Silicon Graphics INDY R5000 computer using InsightII version 95.0 (MSI, Inc.) and the AMBER force field.[27,28] Parameters employed in these studies were the same as those previously described for energy calculations of related platinum model complexes.[17,23,28] Atomic charges of the **Me$_2$ppz** ligand were generated in the CF991 force field (−0.25, −0.08, −0.02, and 0.05 for nitrogens, methyl carbons, methylene carbons, and hydrogen atoms, respectively) and later corrected to reflect platination as previously described.[28] Fifty lowest-energy conformations were generated from energy minimizations and dynamics simulations.[17,23,28]

Results

[Me$_2$ppzPt(9-EtG)$_2$]$^{2+}$. Only one HT H8 signal and one HH H8 signal are expected since the 9-ethyl group is not chiral.[16] The dominant H8 peak is assigned to the HT conformer, and the smaller, more downfield signal is assigned to the HH conformer. (This assignment is based upon conformer distributions and H8 shift patterns observed for other **Me$_2$ppz**Pt**G**$_2$ complexes; i.e., HT forms dominate and the HH conformer exhibits more downfield-shifted H8 signals.) With increasing temperature, these peaks became broader, apparently simultaneously (Supporting Information). Transfer of magnetization was exhibited by the HT signal when the HH signal was irradiated (Figure 3). Minimized energies for the HT and HH rotamers were calculated to be ∼12 and ∼13 kcal/mol, respectively.

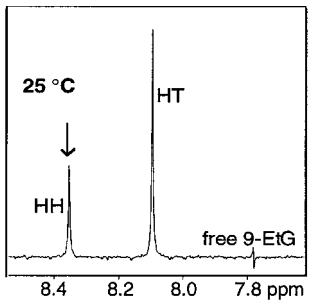

Figure 3. Difference NMR spectrum from a saturation transfer experiment with [**Me$_2$ppz**Pt(9-EtG)$_2$]$^{+2}$, pH 6.2, 25 °C. Arrow indicates irradiated peak.

[Me$_2$ppzPt(Guo)$_2$]$^{2+}$. Four H8 signals assigned to the one HH and the two HT conformers were observed for [**Me$_2$ppz**Pt(Guo)$_2$]$^{2+}$ with a similar distribution at pH 3.3 and 7.0. HT forms (HTa and HTb signals) dominated, and integration of H8 signals revealed only 7% of the HH conformer at pH 7.0 (Table 1). After the pH was raised to 10.0, the HH conformer became undetectable, and the HTa and HTb H8 signals shifted upfield by 0.20 and 0.15 ppm, respectively, consistent with N1H deprotonation (Table 1).[29,30] Minimized energies for all three possible atropisomers of [**Me$_2$ppz**Pt(Guo)$_2$]$^{2+}$ (ΔHT, ΛHT, and HH) were comparable (∼24−25 kcal/mol).

[Me$_2$ppzPt(1-MeGuo)$_2$]$^{2+}$. Four H8 signals were found for [**Me$_2$ppz**Pt(1-MeGuo)$_2$]$^{2+}$. Integration of H8 signals revealed relative percentages at pH 7.0 for the two HT forms and the HH conformer similar to those observed for the Guo analogue (Table 1). No changes in atropisomer distribution or H8 shifts were observed as a function of pH (Table 1).

Me$_2$ppzPt(1-Me-5′-GMP)$_2$. The H8 NMR signals of **Me$_2$ppz**Pt(1-Me-5′-GMP)$_2$ provided evidence for the presence of all three conformers (Figure 4). A dominant HT conformer (HTa signal) was observed at pH 3.0 (Table 1). Approximately equal percentages of the two HT rotamers and the HH conformer were observed at pH 7.4 and 10.0 (Table 1). All four H8 signals shifted downfield as the pH was raised from 3.0 to 7.4 (Table 1), as is commonly observed upon phosphate group deprotonation.[29,31] Cross-peaks between the two most downfield H8 signals (HHd1 and HHd2) were observed in the 2D NOESY spectrum (Figure 5). The two ^{195}Pt NMR resonances observed for **Me$_2$ppz**Pt(1-Me-5′-GMP)$_2$ (−2460 and −2473 ppm) had no significant pH-dependent shift changes, but the intensity of the more downfield signal increased from pH 3.5 to 7.5 (Figure 6).

Me$_2$ppzPt(5′-dGMP)$_2$. H8 shift trends and relative atropisomer ratios observed for **Me$_2$ppz**Pt(5′-dGMP)$_2$ (Supporting Information) were similar to those reported for **Me$_2$ppz**Pt(5′-GMP)$_2$.[22] Similarly, the CD signals of **Me$_2$ppz**Pt(5′-dGMP)$_2$ exhibited behavior identical to that observed for the CD signals of **Me$_2$ppz**Pt(5′-GMP)$_2$ as a function of pH.[22] (At low and neutral pH, the CD signal shape resembled that characteristic of the ΛHT form[15,20,21,23] and then inverted at high pH, Supporting Information.)

(24) Wong, H. C.; Shinozuka, K.; Marzilli, L. G. *Inorg. Chim. Acta* **2000**, *297*, 36−46.
(25) Ciccarese, A.; Clemente, D. A.; Fanizzi, F. P.; Marzotto, A.; Valle, G. *Inorg. Chim. Acta* **1998**, *275*−*276*, 410−418.
(26) Mann, F. G.; Watson, H. R. *J. Chem. Soc.* **1958**, 2772−2780.
(27) Weiner, S.; Kollman, P. A.; Nguyen, D.; Case, D. *J. Comput. Chem.* **1986**, *7*, 230−252.
(28) Yao, S.; Plastaras, J. P.; Marzilli, L. G. *Inorg. Chem.* **1994**, *33*, 6061−6077.
(29) Dijt, F. J.; Canters, G. W.; den Hartog, J. H. J.; Marcelis, A.; Reedijk, J. *J. Am. Chem. Soc.* **1984**, *106*, 3644−3647.
(30) Girault, J.-P.; Chottard, G.; Lallemand, J.-Y.; Chottard, J.-C. *Biochemistry* **1982**, *21*, 1352−1356.
(31) Martin, R. B. *Acc. Chem. Res.* **1985**, *18*, 32−38.

Table 1. Atropisomer Percentage and **G** H8 NMR Chemical Shifts As a Function of pH for **Me$_2$ppz**Pt**G**$_2$ Complexes

complex	pH	HTa % (ppm)	HTb % (ppm)	HH % (ppm)
Me$_2$ppz Pt(5′-GMP)$_2$[a]	3.3	50 (8.37)	26 (8.42)	24 (8.63, 8.73)
	7.4	60 (8.49)	28 (8.47)	12 (8.83, 8.96)
	10.0	29 (8.26)	70 (8.34)	1 (8.76, 8.83)
Me$_2$ppz Pt(3′-GMP)$_2$[b]	3.3	44 (8.40)	48 (8.34)	8 (8.58, 8.63)
	7.5	49 (8.50)	47 (8.35)	4 (8.59, 8.64)
	10.4	38 (8.13)	62 (8.19)	<1 (8.48, 8.54)
Me$_2$ppz Pt(1-Me-5′-GMP)$_2$	3.0	41 (8.29)	31 (8.37)	27 (8.67, 8.74)
	7.4	33 (8.30)	33 (8.44)	34 (8.88, 8.97)
	10.0	33 (8.30)	33 (8.45)	34 (8.91, 8.97)
[**Me$_2$ppz**Pt(Guo)$_2$]$^{2+}$[c]	3.3	45 (8.34)	48 (8.32)	7 (8.55, 8.59)
	7.0	44 (8.31)	49 (8.30)	7 (8.55, 8.59)
	10.0	51 (8.11)	49 (8.15)	not detected
[**Me$_2$ppz**Pt(1-MeGuo)$_2$]$^{2+}$	3.7	43 (8.31)	50 (8.28)	7 (8.57, 8.59)
	7.0	43 (8.31)	50 (8.28)	7 (8.57, 8.59)
	10.3	43 (8.31)	50 (8.28)	7 (8.57, 8.59)
[**Me$_2$ppz**Pt(9-EtG)$_2$]$^{2+}$[d]	6.2	92 (8.15)		8 (8.40)

[a] HT H8 signals exhibit crossover behavior (signals overlap at pH 6.4 and again at pH 9.3). [b] HT H8 signals exhibit crossover behavior at high pH (signals overlap at pH 9.0). [c] HT H8 signals exhibit crossover behavior (overlap at pH 7.4). [d] HTa and HTb cannot be distinguished in this system.

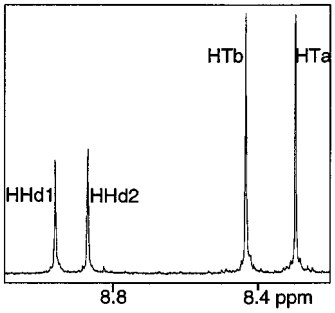

Figure 4. H8 region of ^{1}H NMR spectrum of **Me$_2$ppz**Pt(1-Me-5′-GMP)$_2$, pH 7.4.

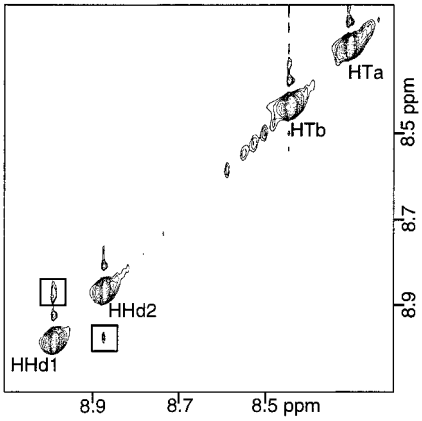

Figure 5. H8 region of 2D NOESY spectrum of **Me$_2$ppz**Pt(1-Me-5′-GMP)$_2$ collected at 5 °C, pH 7.4. Boxes are drawn around NOE cross-peaks.

Me$_2$ppzPt(5′-GMP)$_2$ and Me$_2$ppzPt(3′-GMP)$_2$. Atropisomer percentages and H8 shifts for **Me$_2$ppz**Pt(GMP)$_2$ complexes as a function of pH reported previously[22] are summarized in Table 1. Two ^{195}Pt NMR resonances, at −2471 and −2480 ppm, were observed for **Me$_2$ppz**Pt(5′-GMP)$_2$ at pH 3.4 (Figure 6). Only one signal was observed at pH 7.3 (−2478 ppm); this signal shifted downfield (to −2453 ppm) when the pH was raised to 9.8. For the **Me$_2$ppz**Pt(3′-GMP)$_2$ complex, a dominant ^{195}Pt NMR resonance, at −2484 ppm (Figure 6), shifted downfield as the pH was raised from 7.4 to 9.8. A small shoulder signal (−2470 ppm) was observed only at pH 3.5 for this adduct.

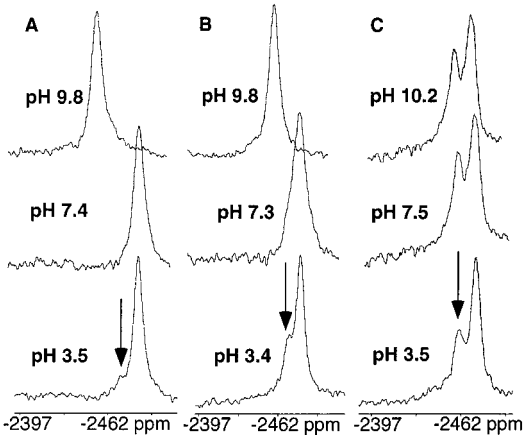

Figure 6. pH dependence of ^{195}Pt NMR spectra of **Me$_2$ppz**Pt(3′-GMP)$_2$ (A), **Me$_2$ppz**Pt(5′-GMP)$_2$ (B), and **Me$_2$ppz**Pt(1-Me-5′-GMP)$_2$ (C). Arrow indicates signal assigned to the HH conformer.

Me$_2$ppzPt(5′-IMP)$_2$. IMP has an H2 signal in addition to the H8 signal. Four H8/H2 sets of NMR signals were observed for **Me$_2$ppz**Pt(5′-IMP)$_2$, pH 3.6 (Supporting Information). The two sets of H8/H2 signals of equal intensity were assigned to the HH conformer; the other two sets were assigned to the HT forms (HTa and HTb signals, Supporting Information). The CD signal of the **Me$_2$ppz**Pt(5′-IMP)$_2$ complex at pH 3.5 exhibited a positive feature at ∼275 nm and a negative feature at ∼245 nm (Supporting Information); this type of CD signal shape has been reported to be characteristic of a ΛHT conformer.[15,20,21,23] Therefore, the dominant form (with the HTa signal) at this pH is ΛHT. The ΛHT form (HTa signal) became more favored when the pH was raised from 3.6 to 7.2. At pH 10.1, the ΔHT (HTb) form was found to dominate (Supporting Information). The CD signal at this pH (∼10) exhibited negative and positive features at ∼295 and ∼255 nm, respectively (Supporting Information); this type of CD signal shape is characteristic of a ΔHT conformer.[15,20,23,24]

Me$_2$ppzPt(3′-IMP)$_2$. NMR signals observed for **Me$_2$ppz**Pt-(3′-IMP)$_2$ were assigned to the three possible atropisomers on the basis of intensity (Supporting Information). An almost equal distribution of the two HT forms was observed at pH 7.3. A very weak CD signal, lacking the characteristic features of either a ΛHT or a ΔHT form, was observed for the **Me$_2$ppz**Pt(3′-

$IMP)_2$ complex at pH ∼3 and ∼7 (Supporting Information). The absence of a characteristic CD signal suggests that at these pH values the ΛHT and ΔHT forms have nearly equal and opposite signal shapes. At pH 10.0, the HH form was not observed and the HT conformer with the HTa signal was the dominant HT form. At this high pH, a CD signal characteristic of a ΛHT form was observed for the **Me$_2$ppz**Pt(3′-IMP)$_2$ complex (Supporting Information). Thus, the dominant HT form (HTa signal) at this pH is assigned as the ΛHT conformer.

Discussion

Conformational Assignments. As found previously,[22] the **Me$_2$ppz**Pt**G**$_2$ adducts have ^{1}H NMR signals indicating the presence of HT and HH rotamers. Two H8 signals of equal intensity (HHd1 and HHd2) observed for **Me$_2$ppz**Pt(5′-GMP)$_2$ and **Me$_2$ppz**Pt(3′-GMP)$_2$ were assigned to the HH rotamer. However, the unusually downfield shifts and small separation between HHd1 and HHd2 prompted us to consider alternative structures, such as an adduct with one **G** bound via N1 and one bound via N7.[22]

The presence of only two H8 signals of unequal intensity for [**Me$_2$ppz**Pt(9-EtG)$_2$]$^{2+}$ provides further evidence that both **G**'s are coordinated by N7 since an N7, N1 species would have two downfield H8 signals of equal intensity even for a **G** such as 9-EtG lacking a chiral ribose. Furthermore, broadening of the two H8 signals at high temperature (Supporting Information) and exchange of magnetization observed in saturation transfer experiments with [**Me$_2$ppz**Pt(9-EtG)$_2$]$^{2+}$ (Figure 3) demonstrate that exchange/interconversion processes undoubtedly involve conformers. Any other interconversion requires Pt−N bond breaking, which is normally very slow.

The NOESY spectrum of **Me$_2$ppz**Pt(1-Me-5′-GMP)$_2$ (Figure 5) shows a cross-peak between the HHd1 and HHd2 signals. Although both NOE and exchange cross-peaks (EXSY) can be present in a NOESY experiment,[16] the HHd1−HHd2 cross-peak is clearly an NOE cross-peak at this low temperature (5 °C) since EXSY cross-peaks between all four H8 signals would have been found otherwise. NOE cross-peaks between H8 signals are characteristic of the HH form.[3,5,13,32] Thus, the 2D NMR data confirm that the observed H8 peaks for these **Me$_2$ppz**Pt**G**$_2$ complexes arise from the HT and HH rotamers.

^{195}Pt NMR signal shifts are sensitive parameters which have often been used to identify the number, type, and geometrical arrangement of the coordinated ligands.[33−36] Only one ^{195}Pt NMR signal was reported for the *cis*-Pt(NH$_3$)$_2$(5′-GMP)$_2$ and **en**Pt(Guo)$_2$ (**en** = ethylenediamine) complexes, at −2455 and −2662 ppm, respectively.[35] However, separate ^{195}Pt signals for the HT forms of **en**Pt(5′-dAMP)$_2$ (5′-dAMP = 2′-deoxyadenosine 5′-monophosphate) were found;[37] therefore, **Me$_2$ppz**Pt**G**$_2$ complexes offered an attractive opportunity to determine if *cis*-PtA_2**G**$_2$ atropisomers could be distinguished by ^{195}Pt NMR spectroscopy.

The ^{195}Pt NMR signals for these **Me$_2$ppz**Pt(GMP)$_2$ adducts, observed between −2484 and −2460 ppm, are similar to those reported for the *cis*-Pt(NH$_3$)$_2$(5′-GMP)$_2$ complex and are consistent with a G N7, G N7-bound adduct.[33,35,38] The very similar ^{195}Pt NMR signal shifts observed for **Me$_2$ppz**Pt(5′-GMP)$_2$ and **Me$_2$ppz**Pt(3′-GMP)$_2$ suggest that the shifts are not dependent on the position of the phosphate group.

At most, only two ^{195}Pt NMR signals were observed for the **Me$_2$ppz**Pt(1-Me-5′-GMP)$_2$, **Me$_2$ppz**Pt(5′-GMP)$_2$, and **Me$_2$ppz**Pt(3′-GMP)$_2$ adducts (Figure 6), although three ^{195}Pt NMR resonances (one for each rotamer) are possible. Fortunately, since these three complexes exhibit different conformer distributions (based on percentages found by ^{1}H NMR spectra) and since these distributions depend on the pH, it was possible to assign definitively the ^{195}Pt NMR peaks. For example, at pH ∼3, the smallest amount of the HH rotamer was observed for **Me$_2$ppz**Pt(3′-GMP)$_2$ (8%, by ^{1}H NMR spectroscopy), whereas significantly larger percentages were found for the **Me$_2$ppz**Pt(5′-GMP)$_2$ (24%) and **Me$_2$ppz**Pt(1-Me-5′-GMP)$_2$ (27%) complexes. This distribution correlates well with the relative intensities of the more downfield ^{195}Pt NMR signal observed for these three adducts at pH ∼3.5 (i.e., whereas a sizable signal was observed for **Me$_2$ppz**Pt(5′-GMP)$_2$ and **Me$_2$ppz**Pt(1-Me-5′-GMP)$_2$, only a small shoulder peak was observed for the **Me$_2$ppz**Pt(3′-GMP)$_2$ complex, Figure 6). In addition, the more downfield ^{195}Pt NMR peak was not observed at pH ∼7 and pH ∼10 for the **Me$_2$ppz**Pt(5′-GMP)$_2$ adduct. However, this more downfield signal increased slightly between pH ∼3 and pH ∼7 and remained constant between pH ∼7 and pH ∼10 for **Me$_2$ppz**Pt(1-Me-5′-GMP)$_2$ (Figure 6); these observations are consistent with the respective decrease/increase in the amount of the HH form as a function of pH indicated by the H8 signals (Table 1). Although we were unable to resolve the ^{195}Pt NMR signals for ΔHT and ΛHT rotamers, we could assign the signal of the HH conformer and distinguish it from the combined signals of the HT forms.

Guanine Base Canting and H8 Shifts. In *cis*-PtA_2**G**$_2$ complexes, **G** base canting may be influenced by the interaction of **G** O6 with the carrier ligand.[11,15,17] Canting could be favored either by repulsive interactions with moieties of the bulky carrier ligands or by attractive interactions with NH groups (Chart 1).

Chart 1. Schematic Representation of a Typical **G** Base (represented by Arrow with H8 at the Head) Canting in an HH Form of *cis*-PtA_2**G**$_2$ Complexes in Which the Carrier Ligand (A_2) Has NH Groups[a]

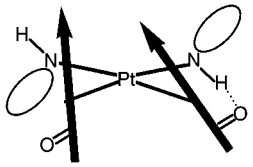

[a] In this figure, the base on the left cants to avoid potential steric clashes between the O6 atom and bulky moieties of the carrier ligand, whereas the base on the right is canted such that the O6 atom can form a hydrogen bond with the carrier-ligand NH group.

Since the **Me$_2$ppz** carrier ligand lacks NH groups and bulky moieties concentrated above/below the platinum coordination plane, potential driving forces that may promote base canting (namely, carrier ligand−**G** O6 steric clashes and carrier ligand−**G** hydrogen bonding) are absent in **Me$_2$ppz**Pt**G**$_2$ complexes. Base canting is more evident in typical HH conformers than in HT rotamers.[15,17] Thus, it is of some interest to assess whether the **G** bases assume a less canted arrangement in the HH conformer of **Me$_2$ppz**Pt**G**$_2$ complexes.

Canting is best assessed using H8 shifts. To assess the unusual H8 chemical shift pattern observed for the HH conformer of **Me$_2$ppz**Pt**G**$_2$ adducts, we analyze first the reason that a large dispersion is normal and second the structures of HH forms

(32) den Hartog, J. H. J.; Altona, C.; van der Marel, G. A.; Reedijk, J. *Eur. J. Biochem.* **1985**, *147*, 371−379.
(33) Bancroft, D. P.; Lepre, C. A.; Lippard, S. J. *J. Am. Chem. Soc.* **1990**, *112*, 6860−6871.
(34) Pregosin, P. S. *Coord. Chem. Rev.* **1982**, *44*, 247−291.
(35) Miller, S. K.; Marzilli, L. G. *Inorg. Chem.* **1985**, *24*, 2421−2425.
(36) Pesek, J. J.; Mason, W. R. *J. Magn. Reson.* **1977**, *25*, 519−529.
(37) Reily, M.; Marzilli, L. G. *J. Am. Chem. Soc.* **1986**, *108*, 6785−6793.
(38) Clore, G. M.; Gronenborn, A. M. *J. Am. Chem. Soc.* **1982**, *104*, 1369−1375.

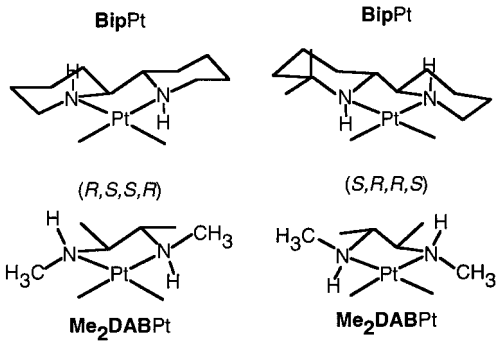

Figure 7. Stick figures of the **Bip**Pt and **Me$_2$DAB**Pt moieties with *R*,*S*,*S*,*R* or *S*,*R*,*R*,*S* chirality. (Stereochemistry defined for the N, C, C, and N ring atoms of the carrier ligand backbone.)

generated from MMD calculations. The ∼1 ppm H8 shift separation commonly observed for the H8 signals of the HH rotamer has been proposed to be related, in part, to the relative canting of the two **G**'s.[15,17] (The canting of one **G** places its H8 atom closer to the anisotropic ring shielding effect of the cis **G**.[39]) For example, the HH form found in **Me$_2$DAB**Pt**G**$_2$ complexes (**Me$_2$DAB** = dimethyl-2,3-diaminobutane, Figure 7) exhibits the large H8 chemical shift dispersion that is commonly observed for this atropisomer.[15] The low-energy HH structures generated for [**Me$_2$DAB**Pt(9-EtG)$_2$]$^{2+}$ showed one **G** canted such that its H8 atom was closer to the five-membered ring of the adjacent base. The anisotropic effects on the H8 shifts of the five- and six-membered rings were estimated[40] for this [**Me$_2$DAB**Pt(9-EtG)$_2$]$^{2+}$ HH model; the canted and uncanted **G**'s were calculated to experience shielding and deshielding effects, respectively. These calculated ring-current effects arising from the canting of only one **G** observed in the HH model of [**Me$_2$DAB**Pt(9-EtG)$_2$]$^{2+}$ help explain the H8 signal shift trend observed for this HH rotamer. However, these calculated ring-current effects do not completely account for the ∼1 ppm H8 signal dispersion observed for the HH form of **Me$_2$DAB**Pt**G**$_2$ complexes (see below).

The HH conformer models generated for [**Me$_2$ppz**Pt(Guo)$_2$]$^{2+}$ and [**Me$_2$ppz**Pt(9-EtG)$_2$]$^{2+}$ support our earlier suggestion[22] that both **G**'s have a similar, less tilted arrangement than the HH form of most other *cis*-PtA$_2$**G**$_2$ complexes. The lowest-energy HH conformer structure for [**Me$_2$ppz**Pt(9-EtG)$_2$]$^{2+}$ had both **G**'s oriented almost perfectly perpendicular to the platinum plane (Chart 2). Both H8 atoms of the [**Me$_2$ppz**Pt(9-EtG)$_2$]$^{2+}$ HH model were calculated[40] to experience a similar, slight *de*shielding (of ∼0.02 ppm). Consequently, the H8 shifts would be similar, as observed, and unlike those in more typical HH conformers of *cis*-PtA$_2$**G**$_2$ adducts, where A$_2$ has NH groups.[15,17] The average H8 shift of both **G**'s of HH conformers in **Me$_2$ppz**Pt**G**$_2$ adducts (8.6 and 8.7 ppm for 3′-GMP and 5′-GMP adducts, respectively, pH ∼3) is more downfield than the average of both **G**'s in a typical HH conformer (8.4 and 8.5 ppm for 3′-GMP and 5′-GMP complexes, respectively, pH ∼3).[15,17]

The magnetic anisotropy of the heavy platinum atom also influences ligand NMR shifts.[11,12,41,42] It was recently proposed that the H8 signal of a **G** base sterically constrained to an orientation closely perpendicular to the coordination plane is

Chart 2. Lowest-Energy Structure for the [**Me$_2$ppz**Pt(9-EtG)$_2$]$^{2+}$ HH Conformer Resulting from MMD Calculations Showing an Uncanted Arrangement of the **G** Bases (9-Et Substituent Omitted for Clarity)

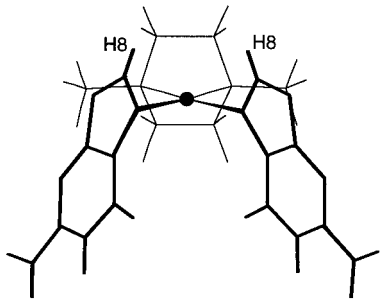

expected to experience a greater deshielding effect due to the magnetic anisotropy of the Pt atom,[12] since in an uncanted (roughly perpendicular) orientation the H8 atom is positioned closer to the *z* axis.[12,41] This Pt anisotropic effect clearly contributes to the downfield-shifted H8 signals of the **Me$_2$ppz**Pt**G**$_2$ HH form since both **G**'s are predicted by modeling to favor a similar, uncanted orientation.

Conformer Distributions. The relative atropisomer stability of *cis*-PtA$_2$**G**$_2$ complexes could depend on several factors. These include amine−**G** O6 or amine−phosphate group hydrogen bonding, steric effects (e.g., clashes between A$_2$ moieties and **G** O6 atoms), and interactions between the two **G** moieties (dipole(**G**)−dipole(**G**) and van der Waals effects, and **G** phosphate group−cis **G** N1H hydrogen bonding).[15,17,20,21,23]

The absence of NH groups in the **Me$_2$ppz** ligand eliminates amine−**G** O6/phosphate group hydrogen bonding as a factor influencing **Me$_2$ppz**Pt**G**$_2$ conformer stabilities. The similar minimized energies calculated for all three [**Me$_2$ppz**Pt(Guo)$_2$]$^{2+}$ atropisomers (∼24−25 kcal/mol) suggest that the absence of a carrier ligand NH group did not destabilize any of the three atropisomers of the [**Me$_2$ppz**Pt(Guo)$_2$]$^{2+}$ complex and, by inference, any rotamers of the other **Me$_2$ppz**Pt**G**$_2$ adducts. These calculations and related ones for [**Me$_2$ppz**Pt(9-EtG)$_2$]$^{2+}$ are consistent with the experimental observations. Moreover, these results support recent work[11,17] indicating that carrier ligand NH−**G** O6 hydrogen bonds have relatively low importance in conformer stabilization. Relating this finding to the anticancer activity of *cis*-PtA$_2$X$_2$ type compounds requires studies of **Me$_2$ppz**Pt adducts with larger nucleic acid fragments.

Dipole(**G**)−dipole(**G**) interactions appear to favor the HT forms over the HH conformer in both solution and solid states,[15] consistent with the observed dominance of the HT rotamers for **Me$_2$ppz**Pt**G**$_2$ adducts. For the **Me$_2$ppz**Pt(5′-GMP)$_2$ and **Me$_2$ppz**-Pt(3′-GMP)$_2$ complexes, "second-sphere" hydrogen-bonding interactions between the phosphate group and the N1H group of the cis **G** were proposed to favor the HT conformers.[22] These interactions are optimal at pH 6−7, conditions in which the phosphate group is deprotonated and the N1 is protonated. The relevance of such interactions is supported by the insensitivity to pH of the HT distributions for complexes in which phosphate group−cis **G** N1H hydrogen bonding is not possible (i.e., **G** = Guo, 1-MeGuo, and 1-Me-5′-GMP, Table 1). Phosphate−cis **G** N1H interactions stabilize the dominant ΛHT (HTa signal) form of **Me$_2$ppz**Pt(5′-GMP)$_2$ relative to the less dominant ΔHT (HTb signal) atropisomer.[22] Thus, the comparable abundance of both HT conformers for the **Me$_2$ppz**Pt(1-Me-5′-GMP)$_2$ complex supports the importance of the phosphate−cis **G** N1H hydrogen-bonding "second-sphere" interaction in stabilizing the dominant HT rotamer.

(39) Kozelka, J.; Fouchet, M. H.; Chottard, J.-C. *Eur. J. Biochem.* **1992**, *205*, 895−906.
(40) Giessner-Prettre, C.; Pullman, B. *Biopolymers* **1976**, *15*, 2277−2286.
(41) Miller, R. G.; Stauffer, R. D.; Fahey, D. R.; Parnell, D. R. *J. Am. Chem. Soc.* **1970**, *92*, 1511−1519.
(42) Sundquist, W. I.; Bancroft, D. P.; Lippard, S. J. *J. Am. Chem. Soc.* **1990**, *112*, 1590−1596.

Increased unfavorable electrostatic interactions between the bases as N1H deprotonates and between the phosphate groups as they deprotonate (PO_4-PO_4 repulsion) were mentioned as possible factors contributing to the decrease in abundance of the HH conformer with increasing pH for the **Me$_2$ppz**Pt(5′-GMP)$_2$ and **Me$_2$ppz**Pt(3′-GMP)$_2$ adducts (Table 1).[22] The HH form was not detected at high pH for [**Me$_2$ppz**Pt(Guo)$_2$]$^{2+}$, whereas the relative percentage of the HH rotamer remained the same between pH ∼7 and ∼10 when N1H deprotonation is not possible (i.e., for [**Me$_2$ppz**Pt(1-MeGuo)$_2$]$^{2+}$ and **Me$_2$ppz**Pt-(1-Me-5′-GMP)$_2$, Table 1). The pH dependence of the three complexes reveals that N1H deprotonation clearly disfavors the HH conformer. Since no decrease in the amount of the HH rotamer was observed from pH 3.0 to pH 7.4 for **Me$_2$ppz**Pt-(1-Me-5′-GMP)$_2$, deprotonation of the phosphate groups does not appear to disfavor the HH conformer. This result indicates that the decrease in the HH form of the **Me$_2$ppz**Pt(5′-GMP)$_2$ and **Me$_2$ppz**Pt(3′-GMP)$_2$ complexes in the pH 3−7 range is due to the increased preference for the HT form resulting from **G** phosphate group−cis **G** N1H interactions (optimal at pH ∼7).

The greatest amount of the HH conformer was found for **Me$_2$ppz**Pt**G**$_2$ adducts with **G**'s bearing a 5′-phosphate group (Table 1). Examination of plastic HH models suggests that the flexibility of the 5′-phosphate group may enable it to hydrogen bond with the **G** 2′-OH, 3′-OH, N1H, or 2-NH_2 moieties. However, the high percentage of the HH rotamer observed for **Me$_2$ppz**Pt(1-Me-5′-GMP)$_2$ suggests that phosphate group−N1H interactions are not important in stabilizing the HH form. Likewise, phosphate group−2′-OH and phosphate group−NH_2 interactions are not solely responsible for increasing the stability of the HH rotamer since similar HH percentages were observed for the **Me$_2$ppz**Pt(5′-GMP)$_2$ (24%), **Me$_2$ppz**Pt(1-Me-5′-GMP)$_2$ (27%), **Me$_2$ppz**Pt(5′-dGMP)$_2$ (21%), and **Me$_2$ppz**Pt(5′-IMP)$_2$ (30%) complexes at low pH (∼3) (Table 1 and Supporting Information).

Slowed Dynamic Motion. The restricted rotation observed for **Me$_2$ppz**Pt**G**$_2$ adducts was also found for the *cis*-PtA$_2$**G**$_2$ models of the chirality-controlling chelate (**CCC**) ligands,[15,17] **Me$_2$DAB** and **Bip** (**Bip** = 2,2′-bipiperidine, Figure 7). As intended by design, these three carrier ligands (**Me$_2$ppz**, **Me$_2$DAB**, and **Bip**) successfully hinder **G** base rotation in their respective *cis*-PtA$_2$**G**$_2$ models relative to models with less bulky carrier ligands. However, the degree by which rotation is slowed appears to be markedly different. For example, whereas EXSY cross-peaks were observed for **Me$_2$DAB**Pt(5′-GMP)$_2$ at 5 °C,[15] no such cross-peaks were observed at this temperature between rotamers of **Me$_2$ppz**Pt(1-Me-5′-GMP)$_2$ (Figure 5). However, saturation transfer was observed between H8 signals of **Me$_2$ppz**Pt-(5′-GMP)$_2$ at 25 and 35 °C,[22] but no such transfer of magnetization was observed between the H8 signals of **Bip**Pt(5′-GMP)$_2$ conformers, even up to 80 °C.[17,18] From these results, **G** base rotation rates of 5′-GMP adducts are inhibited by **Me$_2$ppz** and the **CCC** carrier ligands; however, **Me$_2$ppz** is more effective than **Me$_2$DAB** but less effective than **Bip**.

Another interesting comparison made possible by results from the *cis*-PtA$_2$**G**$_2$ retro models with these three carrier ligands is the dependence of atropisomerization rate on the nature of the N9 substituent of **G**. At room temperature, H8 signals for the [**Me$_2$DAB**(9-EtG)$_2$]$^{2+}$ complex were found to be broader than those observed for the **Me$_2$DAB**(5′-GMP)$_2$ adduct.[15] H8 signals for the 9-EtG and 5′-GMP complexes of the **Me$_2$ppz** and **Bip** carrier ligands were sharp. However, while 1D exchange peaks between H8 signals were observed for both the [**Me$_2$ppz**Pt(9-EtG)$_2$]$^{2+}$ and **Me$_2$ppz**Pt(5′-GMP)$_2$ complexes at 25 °C, such effects were found only for [**Bip**Pt(9-EtG)$_2$]$^{2+}$ at 80 °C, and not for the **Bip**Pt(5′-GMP)$_2$ adduct at this temperature.[17] Thus, this examination of ^{1}H NMR line widths and saturation transfer experiments for the **Me$_2$DAB**Pt**G**$_2$ and **Bip**Pt**G**$_2$ complexes suggests that atropisomerization is faster when **G** = 9-EtG than when **G** = 5′-GMP.[15,17] We attribute the slower rotation rates exhibited by the (**CCC**)Pt(5′-GMP)$_2$ vs the [(**CCC**)Pt(9-EtG)$_2$]$^{2+}$ complexes to hydrogen bonding between the amine hydrogens of the **CCC** carrier ligand and the 5′-phosphate groups. Since the **Me$_2$ppz** ligand lacks amine hydrogens, such interactions are impossible, and atropisomerization rates for [**Me$_2$ppz**Pt(9-EtG)$_2$]$^{2+}$ and **Me$_2$ppz**Pt(5′-GMP)$_2$ are comparable.

Conclusions

The proposed role of **G** phosphate−cis **G** N1H hydrogen bonding in stabilizing the different HT conformers for **Me$_2$ppz**Pt-(5′-GMP)$_2$ and **Me$_2$ppz**Pt(3′-GMP)$_2$[22] is substantiated by the finding of little or no redistribution of the two HT atropisomers as a function of pH in complexes in which such interactions are not possible (**G** = Guo, 1-MeGuo, and 1-Me-5′-GMP). This pH insensitivity contrasts with results for *cis*-PtA$_2$(5′-GMP)$_2$ complexes and is consistent with our proposal that **G** phosphate−cis **G** N1H "second-sphere" hydrogen bonding stabilizes the ΛHT form when **G** = 5′-GMP. One remarkable feature of the **Me$_2$ppz**Pt(1-Me-5′-GMP)$_2$ adduct is that approximately equal amounts of the three atropisomers were observed at pH ∼7 and pH ∼10, suggesting that the less frequently observed HH conformer is comparable in stability to the more commonly found dominant HT forms in this complex. This result with the **Me$_2$ppz**Pt(1-Me-5′-GMP)$_2$ complex clearly indicates that the presence of a 5′-phosphate group favors the HH form. Even in cases of **Me$_2$ppz**Pt(5′-GMP)$_2$ and **Me$_2$ppz**Pt(5′-IMP)$_2$ complexes in which "second-sphere" hydrogen bonding stabilizes the ΛHT form, relatively high amounts of the HH rotamer were found compared to **Me$_2$ppz**Pt**G**$_2$ adducts with **G**'s containing a 3′-phosphate group or no phosphate group. This comparison reinforces our interpretation that the 5′-phosphate group stabilizes the HH atropisomer. Further support for this interpretation comes from some of the early work on 5′-GMP complexes, reporting that the HH form was more abundant than the minor HT conformer.[16] At present, it is not clear how the presence of a 5′-phosphate group overcomes, to some extent, the natural preference for the **G** bases to adopt an HT orientation. The flexible linkage attaching the 5′-phosphate group to the sugar may allow the phosphate groups to engage in multiple inter- and intranucleotide stabilizing interactions; the multiplicity of possible interactions makes it difficult to assess the significance of any single interaction.

Two distinct ^{195}Pt NMR resonances were observed for **Me$_2$ppz**Pt(GMP) complexes: the more downfield signal is assigned to the HH conformer, and the more upfield signal is assigned to both HT forms. *This is the first report of a ^{195}Pt NMR signal for a cis-PtA$_2$**G**$_2$ HH form.* However, since the range of shifts is not large, these resonances may be not be useful for detecting conformers.

HH models generated from MMD calculations on [**Me$_2$ppz**Pt-(9-EtG)$_2$]$^{2+}$ support the NMR data, indicating that the two **G**'s assume a similar, uncanted arrangement in this form. A consistent explanation emerges that Pt magnetic anisotropy causes the unusual H8 chemical shifts exhibited by the HH conformer of **Me$_2$ppz**Pt**G**$_2$ adducts. A corollary implication of this interpretation is that the H8 signal of canted **G** bases can be shifted somewhat upfield by the Pt anisotropy. Thus, the very large dispersion of ∼1 ppm we have reported for HH

conformers in several retro-model systems is caused by both **G** base canting and Pt anisotropy.[11,12,15,17,41,42]

Acknowledgment. This work was supported by NIH Grant GM 29222 (to L.G.M.). We thank Prof. G. Natile (University of Bari) for helpful discussions and MURST, University of Bari, and University of Lecce for financial support also.

Supporting Information Available: H8 region of a [**Me$_2$ppz**Pt(9-EtG)$_2$]$^{2+}$ temperature dependence NMR study; table listing atropisomer percentages and H8 NMR shifts as a function of pH for **Me$_2$ppz**Pt(5′-dGMP)$_2$; table listing atropisomer percentages and chemical shift of H8 and H2 signals as a function of pH for **Me$_2$ppz**Pt(5′-IMP)$_2$ and **Me$_2$ppz**Pt(3′-IMP)$_2$; CD spectra of **Me$_2$ppz**Pt(5′-dGMP)$_2$ recorded at low, neutral, and high pH; CD spectra of **Me$_2$ppz**Pt(IMP)$_2$ adducts; and depictions of the lowest-energy structure of the [**Me$_2$ppz**Pt(9-EtG)$_2$]$^{2+}$ HH conformer resulting from MMD calculations, including a stereoview. This material is available free of charge via the Internet at http://pubs.acs.org.

IC000736X